Photo-CIDNP MAS NMR Studies on photosynthetic reaction centers

Diller, A.

Chapter 1

Introduction

1.1 Photosynthesis

In a classical picture, photosynthesis, performed in algae and higher plants, is the conversion of light energy to chemical energy (Mayer, 1842). Atmospheric carbon dioxide is photochemically reduced to organic material lowering the Gibbs free energy. Shortly after this picture arose, Boltzmann looked upon photosynthesis from a thermodynamics perspective. He observed that plants in their struggle for survival exploit the difference between the energy of sunlight, with low entropy, and the radiation emitted by the earth, with high entropy. In his own words: 'The general struggle for existence of living beings is therefore not a fight for the elements - the elements of all organisms are available in abundance in air, and soil, nor for energy, which is plentiful in the form of heat, unfortunately untransformably, in every body. Rather, it is a struggle for entropy (more accurately: negative entropy) that becomes available through the flow of energy from the hot sun to the cold earth. To make the fullest use of this energy, the plants spread out the immeasurable areas of their leaves and harness the suns energy by a process as yet unexplored, before it sinks down to the temperature level of our earth, to drive chemical syntheses of which one has no inkling as yet in our laboratories. The products of this chemical kitchen are the subject of the struggle in the animal world.' (Boltzmann, 1886). A century later, the science of photosynthesis has grown tremendously. Numerous details in the process of photosynthesis have been unraveled using concepts and techniques from biology, chemistry and physics. Still main aspects of photosynthesis have remained unsolved, such as the water-splitting process of PS II and its unique redox potential. Today, researchers are combining their ideas about photosynthesis to develop synthetic complexes to generate a fuel-like hydrogen from solar energy and water.

1.1.1 Photosystems

The primary processes of photosynthesis are performed by protein-pigment complexes. In photosynthetic bacteria they are located in the cytoplasmic membrane. In plants and cyanobacteria, photosynthesis is driven by two efficient electron pumps embedded in the thylakiod membrane, PS I and PS II (for a review, see (Blankenship, 2002)). According to their terminal electron acceptor photosynthetic organisms are divided into two classes. If the terminal acceptor is a Fe_4S_4 cluster, they belong in the class of type I RCs and in case of quinones to the class of type II RCs (Nitschke and Rutherford, 1991). Non-oxygenic photosynthetic organisms contain only either a type I or type II RC. In plants and cyanobacteria, however, a type I RC and a type II RC, PS I and PS II, are working in series. The antagonistic electrochemical properties of these systems enable an exceptional cooperation (Figure 1.1). The oxidized state of PS II provides a unique force strong enough for water oxidation resulting in the production of atmospheric oxygen. The photochemical excited state of PS I, with its strong reductive power supplies the electrons for the reduction of atmospheric carbon dioxide. Together they constitute the main energy supply of all higher life on earth.

1.1.2 Bacterial reaction centers

The bacterial RC is located in the cytoplasmic membrane and forms together with associated LH complexes the PSU. The LH antennae contain the BChl pigments that capture and funnel the electronic excitation towards the RC, while the RC contains the pigments which directly take part in the photochemical reactions. The bacterial RC has been the first membrane protein of which the three-dimensional structure was determined at an atomic resolution. The RC consists of three protein subunits, M (medium), L (light) and H (heavy), and of nine cofactors. The nine cofactors are 4 BChl *a*, 2 BPhe *a*, 2

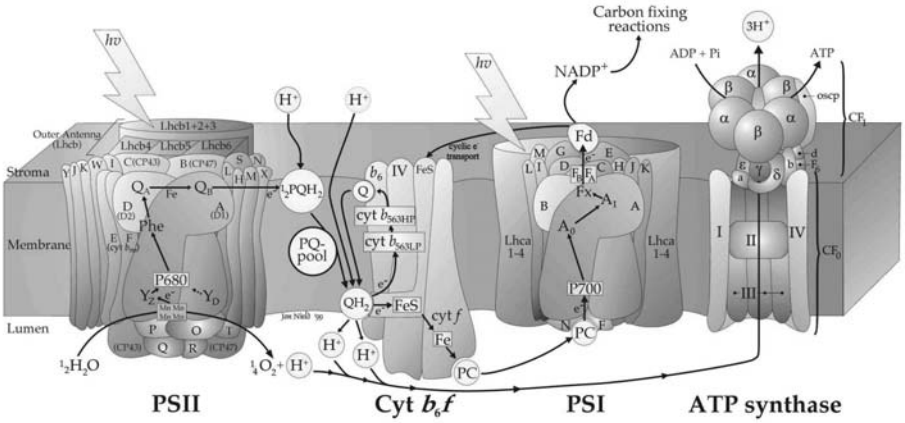

Figure 1.1: Schematic model of the higher plant thylakoid membrane. The main complexes of the membrane, PS II, PS I, the plastoquinone pool, Cyt b_6f and the ATP synthase are shown. The electron transport chain is depicted in black arrows (adapted from Barber, http://www.bio.ic.ac.uk/research/barber/PS IIimages/).

ubiquinone-10, and Fe (Figure 1.2) (Hoff and Deisenhofer, 1997).
The cofactors are arranged in two membrane-spanning branches, A and B. The branches A and B, as well as the L and M subunits are related by a nearly two-fold symmetry. Out of the two available membrane-spanning branches of cofactors, only the A-branch is used to catalyze the photochemical charge separation. NMR chemical shift analysis provides evidence, that the symmetry of the special pair is already broken in its electronic ground sate, although the origin of the symmetry break remains unclear (Schulten *et al.*, 2002; Prakash *et al.*, 2007). This vividly discussed functional asymmetry is not yet understood (Hoff and Deisenhofer, 1997). The electron transfer starts with the donation of an electron from a photoexcited BChl-dimer to an electron transport chain involving monomeric BChl *a*, BPhe *a* and two quinones coupled to an Fe (Woodbury and Allen, 1995). The ratio of A-branch/B-branch electron transfer at room temperature in membrane-bound RCs is estimated to range from 30:1 to 200:1 (Wakeham and Jones, 2005). ENDOR studies have shown that the distribution of the unpaired electron in $P^{+\bullet}$ in the carotenoid-less mutant *Rb. sphaeroides* R-26 is asymmetric, approximately 2:1 in favor of the

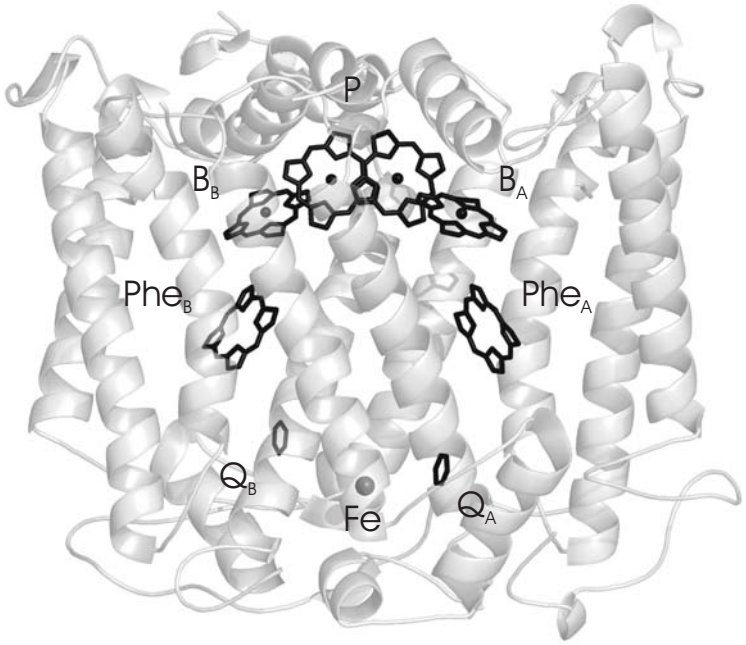

Figure 1.2: Schematic structure of the bacterial RC of *Rb. sphaeroides* obtained with the program PYMOL (DeLano Scientific, South San Francisco, CA). The special pair (P) is a dimer of two BChl molecules. The accessory BChls (B_A, B_B), the BPhe and the ubiquinones (Q_A, Q_B) coupled to an Fe_2, are arranged in a nearly two-fold symmetry (Ermler *et al.*, 1994).

dimer half on the A-branch (Lendzian *et al.*, 1993). Photo-CIDNP MAS NMR studies suggest an electron spin density distribution of 3:2 in favor of the special pair cofactor on the A-branch (Prakash *et al.*, 2005). This is supported by molecular orbital calculations based on the X-ray structure of the RC (Plato *et al.*, 2005). The asymmetry of the electron spin density distribution was shown to depend strongly on the protein surrounding (Rautter *et al.*, 1995; Huber *et al.*, 1996; Käß *et al.*, 1998).

1.1.3 Photosystem I

In the electron transfer chain, PS I has the function of photo-catalyzing the light driven electron transfer from plastocyanin or cytochrome c_6

to ferredoxin. From ferredoxin the electrons get transferred to reduce $NADP^+$ to NADPH, which is used to reduce carbon dioxide in the reactions of the Calvin cycle.

The PS I in plants is a monomer, while the cyanobacterial counterpart assembles *in vivo* into trimers (Chitnis, 2001). The RCs are composed in both cases of several protein subunits, which have the same location and orientation of the electron transfer components. The protein subunits PsaA and PsaB are the most important, since they contain most of the antenna system and cofactors of the electron transport chain from P700, which is a heterodimer formed by one Chl *a* molecule and one Chl *a'* molecule, which is the $C13^2$-epimer of Chl *a*, to the first FeS cluster F_x (Figure 1.3). PsaA and PsaB coordinate also most of the cofactors involved in the electron transport chain (Fromme *et al.*, 2006).

The electron transport chain consists of P700, A (Chl *a*), A_0 (Chl *a*), A_1 (phylloquinone) and the previously mentioned three FeS clusters, F_X, F_A and F_B. F_B is the immediate electron donor to ferredoxin. The midpoint potential of $P700^{+\bullet}$/P700 is about +450 mV placing the excited form, P700*/P700, at about -1.3V, which enables PS I to reduce ferredoxin. In contrast to the bacterial RC the dimeric nature of $P700^{+\bullet}$ is questioned (O'Malley and Babcock, 1984; Webber and Lubitz, 2001). ENDOR and ESEEM measurements on $P700^{+\bullet}$ suggest that this species is a Chl *a* dimer with a strongly asymmetric spin density distribution over the dimer halves, both of which are coordinated by a histidine, which is in analogy to the center Chls of PS II (Käß *et al.*, 1998). According to EPR studies and molecular orbital calculations, there are three H-bonds between Chl *a'* and the protein. This stabilizes Chl *a'* against photooxidation, while the Chl *a* does not form any hydrogen bond to the protein environment. This may cause differences in the redox potential of both Chl molecules and may explain the localization of the unpaired electron of $P700^+$ by more than > 85 % on the active B-branch (Käß *et al.*, 2001; Webber and Lubitz, 2001). Photo-CIDNP studies on PS I also indicate that the unpaired electron is located on a monomeric Chl *a*, which has been tentatively assigned to P2 cofactor (Alia *et al.*, 2004). It has been inferred, that the asymmetry provides a gating of electrons along the two branches (Fromme *et al.*, 2006).

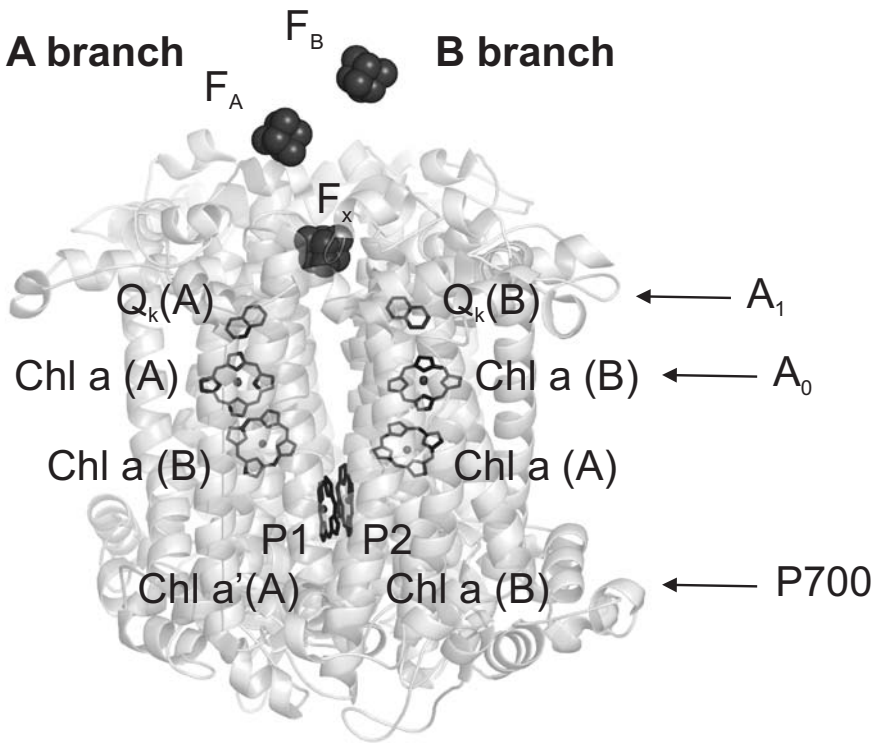

Figure 1.3: Schematic structure of the PS I RC of *Synechococcus elongatus* obtained with the program PYMOL (DeLano Scientific, South San Francisco, CA). The pairs of Chls of the electron transfer chain are arranged in two branches A and B. The description A-branch and B-branch is derived from the protein subunits PsaA and PsaB, respectively. Phylloquinones are marked as Q_k(A) and Q_k(A). The Fe_4S_4 clusters are labeled F_X, F_A and F_B according to their spectroscopic terms (Jordan *et al.*, 2001).

1.1.4 Photosystem II

Inside PS II, light energy is converted into electrochemical potential by the core complex (Figure 1.4). It consists of two homologous proteins D1 and D2, cytochrome *b559*, several small proteins and two Chl *a* binding proteins CP43 and CP47, which serve as an intrinsic antenna system. The peripheral antenna is composed of LH complex II proteins, which contain Chl *a*, Chl *b* and xantophyll molecules. The main function of the antenna proteins is to collect and transfer light

excitation. In addition they are involved in regulatory processes.

A clear picture of the PS II core protein and the antenna arrangement became recently available from X-ray structures, having a resolution of down to 3.0 Å (Zouni *et al.*, 2001; Kamiya and Shen, 2003; Ferreira *et al.*, 2004; Loll *et al.*, 2005). This allows to compare the PS II complex with other oxygenic and anoxygenic photosynthetic RCs. The comparison shows that the D1 and D2 proteins of PS II are not only similar to the L and M subunits of bacterial RCs, but also to the PsaA and PsaB subunits of PS I (Ke and Shuvalov, 1987; Barber, 2003). This illustrates the structural universality among the photosynthetic RCs and the idea that all RCs share a common evolutionary ancestor (Rhee *et al.*, 1998; Schubert *et al.*, 1998).

With respect to the electron transfer all known photosystems posses two branches for the electron transfer. In bacterial RCs as well as PS II only one of them is active. Therefore, in case of PS II, only the D1 protein has to be exchanged upon photodamage, and not the whole core of PS II (Mattoo *et al.*, 1981; Rutherford and Faller, 2003; Shkuropatov *et al.*, 1997, 1999).

1.1.5 Electron transfer in photosystem II

After light excitation, P680 is converted into a strongly reducing agent P680*. Within a picosecond time range the electronic excitation energy of P680* causes the reduction of a Phe molecule. The radical pair state of an oxidized $P680^{+\bullet}$ and $Phe^{-\bullet}$ is formed. The midpoint redox potential of $P680/P680^{+\bullet}$ is experimentally determined to be >1.2V (van Gorkom and Schelvis, 1993). From the Phe the electron travels further down the electron transfer chain, reducing the plastoquinones Q_A and Q_B. After double reduction and protonation Q_B is released from its binding side into the quinone pool located in the thylakoid membrane. The radical pair $P680^{+\bullet}$ is re-reduced by the redox-active tyrosine D1-Tyr161. After four photochemical turnovers four oxidizing equivalents of the S-state cycle are localized on or near the $(Mn)_4$ cluster (Joliot and Kok, 1975).

While the electron transfer chain is clearly defined, the identification of the cofactors of the PS II complex involved in various steps of electron transfer is difficult. However, such functional analysis is very

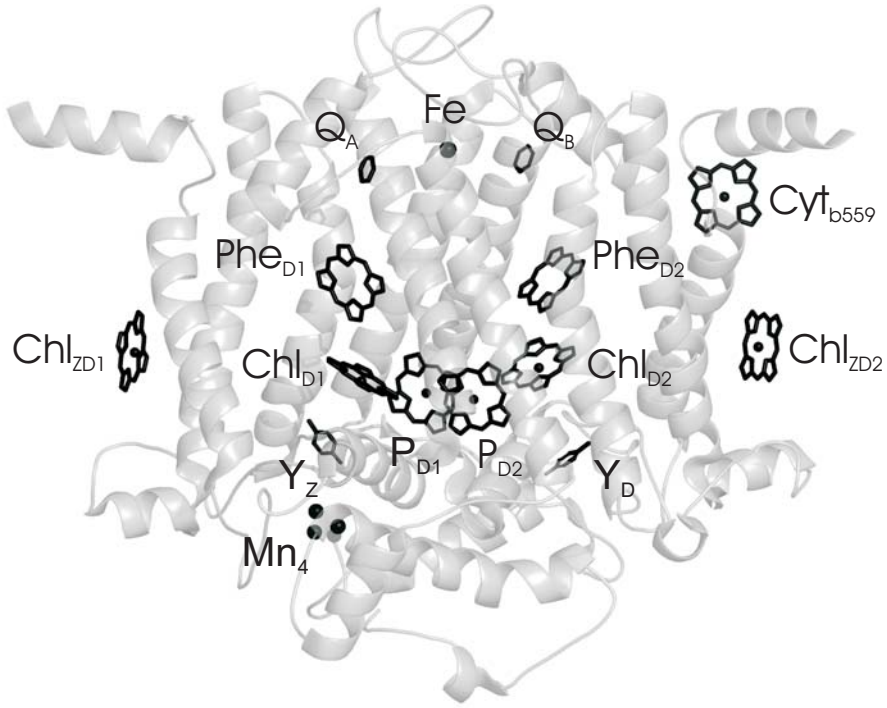

Figure 1.4: Schematic structure of the PS II core complex of *Thermosynechococcus elongatus* obtained with the program PYMOL (DeLano Scientific, South San Francisco, CA). The arrangement of cofactors of the electron transfer chain located in subunits D1 and D2 are Chls P_{D1}, Chl_{D1}, Chl_{ZD1} and Chls P_{D2}, Chl_{D2}, Chl_{ZD2}, respectively. In addition the position of the electron acceptors Q_A and Q_B, and the Fe, as well as the location of Y_D and the Mn_4 cluster, are depicted (Ferreira *et al.*, 2004).

important to understand differences between PS II and other photosystems as well as to extract the principles of photosynthetic electron transfer.

Both, experiments and calculations show, that the excitonic coupling between the chlorins of the D1 and D2 protein of PS II are very similar (Ishikita *et al.*, 2005). Compared with the center Chls of other RCs, P_{D1} and P_{D2} of PS II show a significantly smaller excitonic coupling. The excited state in the PS II RCs is therefore not only localized at the center Chls as in bacterial RCs, but rather delocalized

over the four central Chls and the two Phes, as observed with time-resolved absorption-difference spectroscopy (Durrant *et al.*, 1995; van Brederode and van Grondelle, 1999; Dekker and van Grondelle, 2000; Prokhorenko and Holzwarth, 2000; Diner *et al.*, 2001; Diner and Rappaport, 2002; Renger and Marcus, 2002; Barber, 2003; Frese *et al.*, 2003).

In contrast to the delocalized excited state, EPR experiments show that the triplet state is localized on a single Chl with a chlorin plane tilt of 30° towards the membrane normal (van Mieghem *et al.*, 1991). Detailed calculations of optical properties of the RC are in line with such an assignment, since the only other Chl in the electron chain with a chlorin plane tilt of 30° towards the membrane normal, Chl_{D2}, has a higher site energy, by ≈30 meV (Raszewski *et al.*, 2005). A triplet state on Chl_{D1} results in an efficient quenching of this state by the nearby singly reduced Q_A. This presents a reaction of triplet states with triplet oxygen followed by the formation of physiologically dangerous singlet oxygen (Noguchi *et al.*, 2001; Noguchi, 2002; van Mieghem *et al.*, 1995). At higher temperatures, towards physiological conditions, the triplet is not located on a single Chl, there is a thermally activated hopping of the triplet between Chl_{D1} and P_{D1} (Raszewski *et al.*, 2005).

The charge separation has been believed for a long time to occur from the center Chl, P_{D1}, by analogy with the bacterial RCs, where this step occurs from the special pair. Experiments at low temperature, such as time-resolved infrared spectroscopy at 77 K, confirmed by calculations, show that the initial charge separation occurs not from P_{D1}, but from Chl_{D1} (Noguchi *et al.*, 1993; Durrant *et al.*, 1995; Noguchi *et al.*, 1998; Peterman *et al.*, 1998; Dekker and van Grondelle, 2000; Prokhorenko and Holzwarth, 2000; Diner *et al.*, 2001; Noguchi *et al.*, 2001; Raszewski *et al.*, 2005). Chl_{D1} is then, within 25 ps, reduced by one of the two Chl molecules forming P680 (Prokhorenko and Holzwarth, 2000). The triplet and charge separated state in PS II are therefore not localized on the same Chl cofactor at low temperature, as it is the case for bacterial RCs, where both states are localized on the 'special pair' Chls. Above 20 K both states have been reported to be delocalized over at least two Chls (Ganago *et al.*, 1982; Noguchi *et al.*, 1993; Bosch *et al.*, 1995; van Mieghem *et al.*, 1991; Noguchi

et al., 2001).

1.1.6 Redox potential of photosystem II

The midpoint redox potential of PS II, P680/P680$^{+\bullet}$ of $\sim$+1.2V is very high, compared with the midpoint redox potential of the electron donor of PS I, P700/P700$^{+\bullet}$, +0.4-0.5V and the midpoint redox potential of the special pair in bacterial RCs, P870/P870$^{+\bullet}$ $\sim$+0.5V (Golbeck, 1987; van Gorkom and Schelvis, 1993; Brettel, 1997; Jordan *et al.*, 2001; Ishikita *et al.*, 2005). The lower redox potential of PS I and bacterial RCs restricts these systems to the oxidation of intermediates such as the hemes in cytochromes or the copper in plastocyanines. The redox power of PS II $\sim$+1.2V, is however sufficiently high for the oxidation of water, which requires a minimum value of +0.82 V, and is therewith most important for oxygenic photosynthesis (Ishikita *et al.*, 2005).

Different theories have been developed to explain the increase of 421 mV, reaching from a midpoint redox potential of Chl *a* dissolved in DMF with a potential of +830 mV, to the potential of +1251 mV for P_{D1} found in PS II (Saji and Bard, 1977; Ishikita *et al.*, 2005). The energies of both HOMO and LUMO have to shift equally in the considered theories, to maintain the same energy difference and color. The redox properties of chlorin molecules can be generally affected by ring torsions, according to theoretical predictions a perfectly flat Chl will give rise to the most oxidizing cation (Fajer, 2000).

There is converging evidence that the origin of the oxidizing power of PS II is not due to one effect alone, such as a single mutation, it is rather originated from multiple stepwise processes (Olson and Pierson, 1987; Blankenship and Hartman, 1998; Rutherford and Faller, 2003). Apparently the dielectric environment provided by the RC proteins also plays an important role. Studies on bacterial RCs revealed, that changes in the electrostatic environment of the BChl special pair, mainly through H-bonds, can increase the potential to more than 940 mV, high enough to oxidize tyrosine (Kalman *et al.*, 1999). Analyzing the PS II structure, however, shows no involvement of any H-bonds concerning P_{D1}, P_{D2}, and Chl_{D1} (Ishikita *et al.*, 2005). A very positive electrostatic environment could, however, been provided by a charged

amino acid D2-Arg180 in the neighborhood of the Chl P_{D2}. The counterpart D1-Asn181 on the D1 side is neutral in charge and has little effect on the redox potential (Mulkidjanian, 1999). Point mutations studies of D2-Trp191 which is in van der Waals contact with P_{D2}, suggest that this amino acid can produce an upshift of the redox potential (Keilty *et al.*, 2001). Photo-CIDNP solid-state NMR studies revealed an unexpected shift of the spin density towards ring III of P_{D1}, compared to monomeric Chl *a* in solution with the highest spin density around ring II. A local electrostatic field has been suggested for the stabilization of the HOMO and provided a possible explanation for the high redox potential of $P680^{+\bullet}$. The induced spin density localization around ring III suggests the presence of a local electrostatic field next to the C=O group of ring V (Matysik *et al.*, 2000a).

1.2 Photo-CIDNP MAS NMR

Solid-state MAS NMR is a technique to elucidate structure and function of membrane proteins. An important contribution has been made in the characterization of ligand binding and structure determination of protein-ligand complexes, in the context of research in multidisciplinary fields such as apoptosis or drug discovery and development (Zech *et al.*, 2004; Watts, 2005). One advantage of MAS NMR is that proteins can be analyzed when in the membrane, in the natural environment, or by reconstitution of purified proteins into a membrane. In addition, selective isotope labels can be incorporated at the site of interest to study local structure, *e.g.*, by measuring selected distances or torsion angles (Raleigh *et al.*, 1988; Feng *et al.*, 1996). Proteins incorporated in membranes can be studied also in an oriented form, *e.g.*, to measure helix orientations, or conformation of ligands bound to membrane proteins (Cross and Opella, 1994; Gröbner *et al.*, 2000).

To perform MAS NMR studies on membrane proteins implies the investigation of large systems and therefore improvements to increase the NMR sensitivity are desired. There have been several breakthroughs in this respect, such as isotope enrichment, high magnetic field, and in solid-state NMR the introduction of MAS and cross polarization. Recently, the techniques of DNP, optical pumping and

photo-CIDNP have attracted widespread attention. These techniques have in common that they exploit the much larger magnetic moment of electron spins compared to nuclear spins.

1.2.1 The Photo-CIDNP effect

Photo-CIDNP has been observed in photosynthetic RCs by solid-state under illumination. The photo-CIDNP NMR spectrum contains emissive or absorptive signals with astonishingly high signal amplitudes (Zysmilich and McDermott, 1996b). These high signal amplitudes are due to the fact that CIDNP produces a non-Boltzmann nuclear spin state distribution. The effect is most suitable for the study of photochemical reactions or photophysical processes and is then termed photo-CIDNP. To obtain a maximum of information the underlying mechanisms of photo-CIDNP need to be understood.

Photo-CIDNP has been first observed in solution NMR (Bargon *et al.*, 1967; Bargon and Fischer, 1967; Ward and Lawler, 1967). It is well understood in terms of the radical pair mechanism. The discoverers of this mechanism, Closs and Closs, Kaptein and Oosterhoff described that nuclear spin interactions can alter the recombination probability in reactions that proceed through radical pairs (Closs and Closs, 1969; Kaptein and Oosterhoff, 1969). The radicals forming a singlet radical pair may recombine, while the radicals in a triplet pair are forced to diffuse apart. The application of photo-CIDNP in liquid NMR became a powerful technique to study protein surfaces and effects such as protein-cofactor interactions, conformational changes and denaturation (Hore and Broadhurst, 1993; Goez, 1997).

As diffusion is not significant during the lifetime of the radical pair in the solid-state, the radical pair mechanism cannot occur in frozen proteins. Nevertheless, in 1994, photo-CIDNP has been observed for the first time in solid-state NMR. In these study RCs of *Rb. sphaeroides* were investigated with ^{15}N MAS NMR under continuous illumination with white light (Zysmilich and McDermott, 1994). These studies provide valuable information about primary events in photosynthesis, regarding the electron donor and in some cases also the acceptor and the nearby protein groups. Until now, the solid-state photo-CIDNP effect has been observed in quinone-blocked frozen RCs

of *Rb. sphaeroides* R-26 (Zysmilich and McDermott, 1994, 1996a,b; Matysik *et al.*, 2000b; Prakash *et al.*, 2006) and WT (Schulten *et al.*, 2002; Prakash *et al.*, 2005, 2007), as well as in LH1 RC complexes of *Rps. acidophila* (Diller *et al.*, 2007). Recently, it has been also detected in the RCs of the green sulphur bacterium *Chlorobium tepidum* (Roy *et al.*, 2007). In addition, it has been observed in plant PS I (Alia *et al.*, 2004; Roy *et al.*, 2006) and PS II (Matysik *et al.*, 2000a; Diller *et al.*, 2005).

1.2.2 Photo-CIDNP mechanisms in solids

Figure 1.5 shows the reaction cycle of quinone-blocked RCs, in which forward electron transfer is blocked either by removal or prereduction of the quinone acceptor. Upon photochemical excitation of the electron donor P, an electron is transferred to the primary acceptor A. In quinone reduced or depleted RCs, further electron transfer is blocked. Therefore, the singlet radical pair can either relax to the electronic ground state, or evolve into a triplet radical pair. The triplet radical pair recombines to a donor triplet ^{3}P and an acceptor singlet. Finally, the donor triplet relaxes to the singlet ground state, so that the whole process is cyclic and hence no net effect on the nuclei would be expected due to the branching of the reaction pathway. Scheme 1.5 indicates and briefly explains the three mechanisms that can be simultaneously involved to create symmetry breaking and build up net nuclear polarization: TSM, DD and DR (Jeschke and Matysik, 2003; Daviso *et al.*, 2007).

For the following approach a simple spin system is considered, composed of two coupled electron spins, $S_1 = 1/2$, $S_2 = 1/2$ and one nuclear spin, $I = 1/2$, that is hyperfine coupled to S_1. In photo-CIDNP net nuclear polarization is due to a conversion of electron-electron zero quantum coherence into nuclear polarization I_z. The TSM contribution is strongest at the matching condition $|A| \approx 2|d| \approx 2|\omega_I|$, with $A = A_{zz} = a_{\mathrm{iso}} + T(3\ \cos^2\ \theta_{\mathrm{hfi}}\text{-}1)$ the secular hyperfine interaction, T the hyperfine tensor in the principal axis frame, d the electron-electron coupling and ω_I the nuclear Zeeman frequency (Jeschke, 1997, 1998; Jeschke and Matysik, 2003). The matching leads to polarization transfer mediated by the pseudosecular part of the *hf* interaction, B

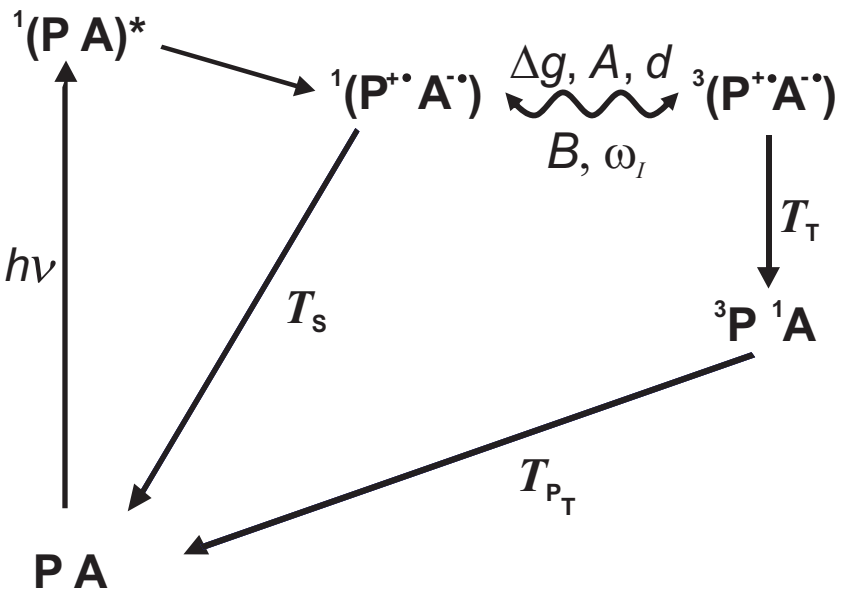

Figure 1.5: Reaction cycle in quinone-blocked RCs. The oscillating arrow represents coherent evolution of the initial pure singlet state into a triplet radical pair and back, which is a complex process due to the difference of the g value between the two electrons, Δg, the secular part of the hf interaction, A, the coupling between the two electrons, d, the pseudo-secular hyperfine coupling, B, and the nuclear Zeeman frequency, ω_I. Three mechanism are known to build up net nuclear polarization in the solid-state: the TSM, the DD and the DR mechanism. The TSM contribution is strongest at the matching condition $|A| \approx 2|d| \approx 2|\omega_I|$. In the DD mechanism, the formation of net nuclear polarization is based on different lifetimes of the singlet and the triplet pairs, T_{S} and T_{T}, respectively. In the DR, net nuclear polarization is thought to arise from opposite polarization in singlet and triplet radical pairs that do not cancel since part of the triplet-derived polarization relaxes during the triplet lifetime, $T_{\mathrm{P_T}}$ (McDermott *et al.*, 1998). This requires that the longitudinal relaxation time of the nuclei in the RC triplet is shortened to such an extent that it is comparable to $T_{\mathrm{P_T}}$ (Jeschke and Matysik, 2003; Daviso *et al.*, 2007). The direction of the excitation and decay after light-induced electron transfer from the electron donor (P) to the primary acceptor (A), are shown in solid arrows.

$=\sqrt{A_{zx}^2 + A_{zy}^2}$, which is for ^{13}C 5-10 MHz. Overall transfer is proportional to B^2 and takes place with a polarization rate within the lifetime of the correlated radical pair, which is on a nanosecond time scale .

In the DD mechanism, the formation of net nuclear polarization is based on different lifetimes of the singlet, $^1(P^{+\bullet}A^{-\bullet})$, and the triplet, $^3(P^{+\bullet}A^{-\bullet})$, radical pairs (Polenova and McDermott, 1999). In contrast to the TSM, electron-electron coupling is not required although the anisotropic *hf* coupling is still indispensable (Jeschke and Matysik, 2003). For both coherent mechanisms, the TSM and DD mechanism, based on anisotropic interactions, an orientational dependence of photo-CIDNP is expected. Chapter 6 will explore this orientational dependence in some detail.

In addition to TSM and DD, a third mechanism named DR can occur. In the DR, the symmetry breaking between the two decay branches from singlet and triplet radical pairs and the production of net nuclear polarization has been attributed to a fast nuclear spin lattice relaxation caused by the triplet state of the donor (Prakash *et al.*, 2005, 2006). Nuclear polarization from triplet pairs partially decays during the lifetime of the donor triplet, ^3P (Goldstein and Boxer, 1987; McDermott *et al.*, 1998). During this long lifetime the triplet opens up relaxation channels that can contribute to establish net nuclear polarization. This is explained further in Chapter 2.

The photo-CIDNP spectrum of WT RCs, which entirely shows emissive signals, has been explained in terms of parallel running TSM and DD mechanisms (Prakash *et al.*, 2005). In RCs of the carotenoidless mutant R-26, the triplet lifetime is around 30 μs (Parson *et al.*, 1975). If one compares the polarization pattern of WT and R-26 RCs, one observes a sign change for signals assigned to the special pair. The difference in polarization can be explained by a contribution of DR. It is an incoherent process and the magnitude can be as large as induced by the other two mechanisms (see Chapter 6).

1.3 Aim and scope of the thesis

In this thesis advantages of photo-CIDNP MAS NMR, such as faster scanning and spectral editing are demonstrated. The main aim is to show how photo-CIDNP MAS NMR can be applied to plant photosystems in order to develop a model for the donor of PS II and address the origin of the highest redox potential found in a living system.

Chapter 2 describes how the same processes creating net polarization in photo-CIDNP opens up light-dependent channels for polarization losses. This leads to coherently and incoherently enhanced signal recovery, additional to the recovery due to light-independent longitudinal relaxation. It is presented how photo-CIDNP MAS NMR provides a possibility to drive NMR technique beyond the T_1 relaxation time expected for frozen proteins.

The extraordinary high redox potential for PS II is discussed in **Chapter 3**. Based on a comparison between photo-CIDNP MAS NMR data of PS I and PS II, a local electrostatic field caused by matrix involvement as the origin for the high redox potential is suggested.

The underlying concept of the electrostatic field is based on the comparison of the electron spin distribution in PS I and PS II. ^{15}N-photo-CIDNP MAS NMR presented in **Chapter 4** provides a clear comparison between the electron spin distribution found in PS I and PS II. The electron spin density in case of PS II is inverted compared to PS I or isolated Chls. A model for the donor of PS II is presented explaining the inversion of electron spin density based on a tilt of the axial histidine towards pyrrole ring IV causing π-π overlap of both aromatic systems.

Chapter 5 presents photo-CIDNP experiments on selectively isotope labeled purified RCs as well as membrane bound RCs from the WT of *Rb. sphaeroides*. Isotope labeling provides an additional gain in NMR sensitivity and selectivity. While photo-CIDNP experiments on selectively isotope labeled purified RCs show no influence on the sign of the photo-CIDNP effect, the sign of the photo-CIDNP effect of membrane bound RCs shows an inversion and appear as absorptive (positive) signals upon isotope labeling. A possible origin of the sign-change effect is discussed and shows how the sign-change effect allows to distinguish between donor signals and acceptor signals and can be employed for spectral editing.

Chapter 6 provides general conclusions and prospects of photo-CIDNP MAS NMR and suggests future applications.

Bibliography

Alia, Roy, E., Gast, P., van Gorkom, H. J., de Groot, H. J. M., Jeschke, G., and Matysik, J. (**2004**) Photochemically Induced Dynamic Nuclear Polarization in Photosystem I of Plants Observed by ^{13}C Magic-Angle Spinning NMR. *J Am Chem Soc* 126: 12819–12826.

Barber, J. (**2003**) Photosystem II: The Engine of Life. *Quart Rev Biophys* 36: 71–89.

Bargon, J., and Fischer, H. (**1967**) Kernresonanz-Emissionslinien während rascher Radikalreaktionen. 2. Chemisch induzierte Dynamische Kernpolarisation. *Z Naturforsch* A 22: 1556–1562.

Bargon, J., Fischer, H., and Johnsen, U. (**1967**) Kernresonanz-Emissionslinien während rascher Radikalreaktionen. I. Aufnahmeverfahren und Beispiele. *Z Naturforsch* A 22: 1551–1555.

Blankenship, R. E. (**2002**): Molecular Mechanisms of Photosynthesis. Blackwell Science, Oxford.

Blankenship, R. E., and Hartman, H. (**1998**) The Origin and Evolution of Oxygenic Photosynthesis. *Trends Biochem* 23: 94–97.

Boltzmann, L. (**1886**) Populäre Schriften. Barth Verlag, Leipzig (1905).

Bosch, M. K., Proskuryakov, I. I., Gast, P., and Hoff, A. J. (**1995**) Relative Orientation of the Optical Transition Dipole and Triplet Axes of the Photosystem II Primary Donor. A Magnetophotoselection Study. *J Phys Chem* 99: 15310–15316.

Brettel, K. (**1997**) Electron Transfer and Arrangement of the Redox Cofactors in Photosystem I. *Biochim Biophys Acta* 1318: 322–373.

Chitnis, P. R. (**2001**) Photosystem I: Function and Physiology. *Annu Rev Plant Biol* 52: 593–626.

Closs, G. L., and Closs, L. E. (**1969**) Induced Dynamic Nuclear Spin Polarization in Reactions of Photochemically and Thermally Generated Triplet Diphenylmethylene. *J Am Chem Soc* 91: 4549–4550.

Cross, T. A., and Opella, S. J. (**1994**) Solid-State NMR Structural Studies of Peptides and Proteins in Membranes. *Curr Opin Struct Biol* 4: 574–581.

Daviso, E., Jeschke, G., and Matysik, J. (**2007**) Photochemically Induced Dynamic Nuclear Polarization (Photo-CIDNP) Magic-Angle Spinning NMR. *In* Biophysical Techniques in Photosynthesis II. Aartsma, T. J. and Matysik, J., eds., Springer, Dordrecht, pp. 385-399.

Dekker, J. P., and van Grondelle, R. (**2000**) Primary Charge Separation in Photosystem II. *Photosynth Res* 63: 195–208.

Diller, A., Alia, Roy, E., Gast, P., van Gorkom, H. J., Zaanen, J., de Groot,

H. J. M., Glaubitz, C., and Matysik, J. (**2005**) Photo-CIDNP Solid-State NMR on Photosystems I and II: What Makes P680 Special? *Photosynth Res* 84: 303–308.

Diller, A., Alia, A., Gast, P., Jeschke, G., and Matysik, J. (**2007**) ^{13}C Photo-CIDNP MAS NMR on the LH1-RC complex of *Rhodopseudomonas acidophila*. *In* Proceedings of the 14th International Congress on Photosynthesis. Allen, J. F., Gantt, E., Golbeck, J. H. and Osmond, B., eds., Springer, Dordrecht, submitted.

Diner, B. A., and Rappaport, F. (**2002**) Structure, Dynamics, and Energetics of the Primary Photochemistry of Photosystem II of Oxygenic Photosynthesis. *Annu Rev Plant Biol* 53: 551–580.

Diner, B. A., Schlodder, E., Nixon, P. J., Coleman, W. J., Rappaport, F., Lavergne, J., Vermaas, W. F. J., and Dexter, D. A. (**2001**) Site-directed Mutations at D1-His198 and D2-His197 on Photosystem II in *Synechocystis* PCC 6803: Sites of Primary Charge Separation and Cation and Triplet Stabilisation. *Biochemistry* 40: 9265–9281.

Durrant, J. R., Klug, D. R., Kwa, S. L. S., van Grondelle, R., Porter, G., and Dekker, J. P. (**1995**) A Multimer Model for P680, the Primary Electron-Donor of Photosystem II. *Proc Natl Acad Sci USA* 92: 4798–4802.

Ermler, U., Fritzsch, G., Buchanan, S. K., and Michel, H. (**1994**) Structure of the Photosynthetic Reaction Center from *Rhodobacter sphaeroides* at 2.65 Ångstrom Resolution: Cofactors and Protein-Cofactor Interactions. *Structure* 2: 925–936.

Fajer, J. (**2000**) Structural Effects in Chemistry and Biology. *J Porphyrins Phthalocyanines* 4: 382–385.

Feng, X., Lee, Y. K., Sandström, D., Eden, M., Maisel, H., Sebald, A., and Levitt, M. H. (**1996**) Direct Determination of a Molecular Torsional Angle by Solid-State NMR. *Chem Phys Lett* 257: 314–320.

Ferreira, K. N., Iverson, T. M., Maghlaoui, K., Barber, J., and Iwata, S. (**2004**) Architecture of the Photosynthetic Oxygen-Evolving Center. *Science* 303: 1831–1838.

Frese, R. N., Germano, M., de Weerd, F. L., van Stokkum, I. H. M., Shkuropatov, A. Y., Shuvalov, V. A., van Gorkom, H. J., van Grondelle, R., and Dekker, J. P. (**2003**) Electric Field Effects on the Chlorophylls, Pheophytins, and β-Carotenes in the Reaction Center of Photosystem II. *Biochemistry* 42: 9205–9213.

Fromme, P., Yu, H. Q., de Ruyter, Y. S., Jolley, C., Chauhan, D. K., Melkozernov, A., and Grotjohann, I. (**2006**) Structure of Photosystems

I and II. *C R Chimie* 9: 188–200.

Ganago, I. B., Klimov, V. V., Ganago, A. O., Shuvalov, V. A., and Erokhin, Y. E. (**1982**) Linear Dichroism and Orientation of Pheophytin, the Intermediary Electron Acceptor in Photosystem II Reaction Centers. *FEBS Lett* 140: 127–130.

Goez, M. (**1997**) Photochemically Induced Dynamic Nuclear Polarization. *Advanc Photochem* 23: 63–164.

Golbeck, J. H. (**1987**) Structure, Function and Organization of the Photosystem I Reaction Center Complex. *Biochim Biophys Acta* 895: 167–204.

Goldstein, R. A., and Boxer, S. G. (**1987**) Effects of Nuclear-Spin Polarization on Reaction Dynamics in Photosynthetic Bacterial Reaction Centers. *Biophys J* 51: 937–946.

Gröbner, G., Burnett, I. J., Glaubitz, C., Choi, G., Mason, A. J., and Watts, A. (**2000**) Observations of Light-Induced Structural Changes of Retinal within Rhodopsin. *Nature* 405: 810–813.

Hoff, A. J., and Deisenhofer, J. (**1997**) Photophysics of Photosynthesis. Structure and Spectroscopy of Reaction Centers of Purple Bacteria. *Phys Rep* 287: 2–247.

Hore, P. J., and Broadhurst, R. W. (**1993**) Photo-CIDNP of Biopolymers. *Progr Nucl Magn Reson Spectrosc* 25: 345–402.

Huber, M., Isaacson, R. A., Abresch, E. C., Gaul, D., Schenck, C. C., and Feher, G. (**1996**) Electronic Structure of the Oxidized Primary Electron Donor of the HL (M202) and HL (L173) Heterodimer Mutants of the Photosynthetic Bacterium *Rhodobacter sphaeroides*: ENDOR on Single Crystals of Reaction Centers. *Biochim Biophys Acta* 1273: 108–128.

Ishikita, H., Loll, B., Biesiadka, J., Saenger, W., and Knapp, E. W. (**2005**) Redox Potentials of Chlorophylls in the Photosystem II Reaction Center. *Biochemistry* 44: 4118–4124.

Jeschke, G. (**1997**) Electron-Electron-Nuclear Three-Spin Mixing in Spin-Correlated Radical Pairs. *J Chem Phys* 106: 10072–10086.

Jeschke, G. (**1998**) A New Mechanism for Chemically Induced Dynamic Nuclear Polarization in the Solid State. *J Am Chem Soc* 120: 4425–4429.

Jeschke, G., and Matysik, J. (**2003**) A Reassessment of the Origin of Photochemically Induced Dynamic Nuclear Polarization Effects in Solids. *Chem Phys* 294: 239–255.

Joliot, P., and Kok, B. (**1975**) Oxygen Evolution in Photosynthesis. *In* Bioenergetics and Photosynthesis. Govindjee, ed., Academic, New York, pp 387-412.

Jordan, P., Fromme, P., Witt, H. T., Klukas, O., Saenger, W., and Krauss,

N. (**2001**) Three-Dimensional Structure of Cyanobacterial Photosystem I at 2.5 Å Resolution. *Nature* 411: 909–917.

Kalman, L., LoBrutto, R., Allen, J. P., and Williams, J. C. (**1999**) Modified Reaction Centres Oxidize Tyrosine in Reactions that Mirror Photosystem II. *Nature* 402: 696–699.

Kamiya, N., and Shen, J. R. (**2003**) Crystal Structure of Oxygen-Evolving Photosystem II from *Thermosynechococcus vulcanus* at 3.7 Å Resolution. *Proc Natl Acad Sci USA* 100: 98–103.

Kaptein, R., and Oosterhoff, J. L. (**1969**) Chemically Induced Dynamic Nuclear Polarization II (Relation with Anomalous ESR Spectra). *Chem Phys Lett* 4: 195–197.

Käß, H., Fromme, P., Witt, H. T., and Lubitz, W. (**2001**) Orientation and Electronic Structure of the Primary Donor Radical Cation $P700^{+\bullet}$ in Photosystem I: A Single Crystals EPR and ENDOR Study. *J Phys Chem B* 105: 1225–1239.

Käß, H., Lubitz, W., Hartwig, G., Scheer, H., Noy, D., and Scherz, A. (**1998**) ENDOR Studies of Substituted Chlorophyll Cation Radicals. *Spectrochim Acta* 54: 1141–1156.

Ke, B., and Shuvalov, V. A. (**1987**) Picosecond Fluorescence Spectroscopy and Energy Transfer in Photosynthetic Antenna Pigments. *In* The Light Reactions. Barber J., ed., Elsevier, Amsterdam, pp 95-157.

Keilty, A. T., Vavilin, D. V., and Vermaas, W. F. J. (**2001**) Functional Analysis of Combinatorial Mutants with Changes in the C-Terminus of the CD Loop of the D2 Protein in Photosystem II of *Synechocystis* sp. PCC 6803. *Biochemistry* 40: 4131–4139.

Lendzian, F., Huber, M., Isaacson, R. A., Endeward, B., Plato, M., Bönigk, B., Möbius, K., Lubitz, W., and Feher, G. (**1993**) The Electronic-Structure of the Primary Donor Cation-Radical in *Rhodobacter sphaeroides* R26: ENDOR and Triple-Resonance Studies in Single-Crystals of Reaction Centers. *Biochim Biophys Acta* 1183: 139–160.

Loll, B., Kern, J., Saenger, W., Zouni, A., and Biesiadka, J. (**2005**) Towards Complete Cofactor Arrangement in the 3.0 Å Resolution Structure of Photosystem II. *Nature* 438: 1040–1044.

Mattoo, A. K., Pick, U., Hoffmanfalk, H., and Edelman, M. (**1981**) The Rapidly Metabolized 32,000-Dalton Polypeptide of the Chloroplast is the "Proteinaceous Shield" Regulating Photosystem II Electron-Transport and Mediating Diuron Herbicide Sensitivity. *Proc Natl Acad Sci USA* 78: 1572–1576.

Matysik, J., Alia, Gast, P., van Gorkom, H. J., Hoff, A. J., and de Groot,

H. J. M. (**2000a**) Photochemically Induced Nuclear Spin Polarization in Reaction Centers of Photosystem II Observed by ^{13}C Solid-State NMR Reveals a Strongly Asymmetric Electronic Structure of the $P680^{+\bullet}$ Primary Donor Chlorophyll. *Proc Natl Acad Sci USA* 97: 9865–9870.

Matysik, J., Alia, Hollander, J. G., Egorova-Zachernyuk, T., Gast, P., and de Groot, H. J. M. (**2000b**) A Set-Up to Study Photochemically Induced Dynamic Nuclear Polarization in Photosynthetic Reaction Centres by Solid-State NMR. *Indian J Biochem Biophys* 37: 418–423.

Mayer, J. R. (**1842**) Bemerkungen über die Kräfte der Unbelebten Natur. *Ann Chem und Pharm* 42: 233–240.

McDermott, A., Zysmilich, M. G., and Polenova, T. (**1998**) Solid State NMR Studies of Photoinduced Polarization in Photosynthetic Reaction Centers: Mechanism and Simulations. *Solid State Nucl Mag Res* 11: 21–47.

Mulkidjanian, A. Y. (**1999**) Photosystem II of Green Plants: On the Possible Role of Retarded Protonic Relaxation in Water Oxidation. *Biochim Biophys Acta* 1410: 1–6.

Nitschke, W., and Rutherford, A. W. (**1991**) Photosynthetic Reaction Centres: Variations on a Common Structural Theme. *Trends Biochem Sci* 16: 241–245.

Noguchi, T. (**2002**) Dual Role of Triplet Localization on the Accessory Chlorophyll in the Photosystem II Reaction Center: Photoprotection and Photodamage of the D1 Protein. *Plant Cell Physiol* 43: 1112–1116.

Noguchi, T., Inoue, Y., and Satoh, K. (**1993**) FT-IR Studies on the Triplet State of P680 in the Photosystem II Reaction Center: Triplet Equilibrium within a Chlorophyll Dimer. *Biochemistry* 32: 7186–7195.

Noguchi, T., Tomo, T., and Inoue, Y. (**1998**) Fourier Transform Infrared Study of the Cation Radical of P680 in the Photosystem II Reaction Center: Evidence for Charge Delocalization on the Chlorophyll Dimer. *Biochemistry* 37: 13614–13625.

Noguchi, T., Tomo, T., and Kato, C. (**2001**) Triplet Formation on a Monomeric Chlorophyll in the Photosystem II Reaction Center as Studied by Time-Resolved Infrared Spectroscopy. *Biochemistry* 40: 2176–2185.

Olson, J. M., and Pierson, B. K. (**1987**) Origin and Evolution of Photosynthetic Reaction Centers. *Orig Life Evol Biosph* 17: 419–430.

O'Malley, P. J., and Babcock, G. T. (**1984**) Electron Nuclear Double Resonance Evidence Supporting a Monomeric Nature for $P700^{+}$ in Spinach Chloroplasts. *Proc Natl Acad Sci USA* 81: 1098–1101.

Parson, W. W., Clayton, R. K., and Cogdell, R. J. (**1975**) Excited-States of Photosynthetic Reaction Centers at Low Redox Potentials. *Biochim Biophys Acta* 387: 265–278.

Peterman, E. J. G., van Amerongen, H., van Grondelle, R., and Dekker, J. P. (**1998**) The Nature of the Excited State of the Reaction Center of Photosystem II of Green Plants: A High Resolution Fluorescence Spectroscopy Study. *Proc Natl Acad Sci USA* 95: 6128–6133.

Plato, M., Möbius, K., and Lubtiz, W. (**2005**) Molecular Orbital Calculations on Chlorophyll Radical Ions. *In* Chlorophylls. Scheer, H., ed., CRC Press, Boca Raton, pp 1015-1046.

Polenova, T., and McDermott, A. E. (**1999**) A Coherent Mixing Mechanism Explains the Photoinduced Nuclear Polarization in Photosynthetic Reaction Centers. *J Phys Chem B* 103: 535–548.

Prakash, S., Alia, Gast, P., de Groot, H. J. M., Jeschke, G., and Matysik, J. (**2005**) Magnetic Field Dependence of Photo-CIDNP MAS NMR on Photosynthetic Reaction Centers of *Rhodobacter sphaeroides* WT. *J Am Chem Soc* 127: 14290–14298.

Prakash, S., Alia, Gast, P., de Groot, H. J. M., Jeschke, G., and Matysik, J. (**2007**) ^{13}C Chemical Shift Map of the Active Cofactors in Photosynthetic Reaction centers of *Rhodobacter sphaeroides* Revealed by Photo-CIDNP MAS NMR. *Biochemistry* 46: 8953–8960.

Prakash, S., Alia, Gast, P., de Groot, H. J. M., Matysik, J., and Jeschke, G. (**2006**) Photo-CIDNP MAS NMR in Intact Cells of *Rhodobacter sphaeroides* R26: Molecular and Atomic Resolution at Nanomolar Concentration. *J Am Chem Soc* 128: 12794–12799.

Prokhorenko, V. I., and Holzwarth, A. R. (**2000**) Primary Processes and Structure of the Photosystem II Reaction Center: A Photon Echo Study. *J Phys Chem B* 104: 11563–11578.

Raleigh, D. P., Levitt, M. H., and Griffin, R. G. (**1988**) Rotational Resonance in Solid-State NMR. *Chem Phys Lett* 146: 71–76.

Raszewski, G., Saenger, W., and Renger, T. (**2005**) Theory of Optical Spectra of Photosystem II Reaction Centers: Location of the Triplet State and the Identity of the Primary Electron Donor. *Biophys J* 88: 986–998.

Rautter, J., Lendzian, F., Schulz, C., Fetsch, A., Kuhn, M., Lin, X., Williams, J. C., Allen, J. P., and Lubitz, W. (**1995**) ENDOR Studies of the Primary Donor Cation Radical in Mutant Reaction Centers of *Rhodobacter sphaeroides* with Altered Hydrogen-Bond Interactions. *Biochemistry* 34: 8130–8143.

Renger, T., and Marcus, R. A. (**2002**) On the Relation of Protein Dynamics and Exciton Relaxation in Pigment-Protein Complexes: An Estimation of the Spectral Density and a Theory for the Calculation of Optical Spectra. *J Chem Phys* 116: 9997–10019.

Rhee, K. H., Morris, E. P., Barber, J., and Kühlbrandt, W. (**1998**) Three-dimensional Structure of the Plant Photosystem II Reaction Centre at 8 Å Resolution. *Nature* 396: 283–286.

Roy, E., Alia, Gast, P., van Gorkom, H. J., de Groot, H. J. M., Jeschke, G., and Matysik, J. (**2007**) Photochemically Induced Dynamic Nuclear Polarization in the Reaction Center of the Green Sulphur Bacterium *Chlorobium tepidum* Observed by ^{13}C MAS NMR. *Biochim Biophys Acta* 1767: 610–615.

Roy, E., Diller, A., Alia, A., Gast, P., van Gorkom, H. J., de Groot, H. J. M., Jeschke, G., and Matysik, J. (**2006**) Magnetic Field Dependence of ^{13}C Photo-CIDNP MAS NMR in Plant Photosystems I and II. *Appl Magn Reson* 31: 193–204.

Rutherford, A. W., and Faller, P. (**2003**) Photosystem II: Evolutionary Perspectives. *Philos Trans R Soc Lond, B* 358: 245–253.

Saji, T., and Bard, A. J. (**1977**) Electrogenerated Chemiluminescence. 29. Electrochemistry and Chemiluminescence of Chlorophyll *a* in *N,N*-Dimethylformamide Solutions. *J Am Chem Soc* 99: 2235–2240.

Schubert, W. D., Klukas, O., Saenger, W., Witt, H. T., Fromme, P., and Krauss, N. (**1998**) A Common Ancestor for Oxygenic and Anoxygenic Photosynthetic Systems: A Comparison Based on the Structural Model of Photosystem I. *J Mol Biol* 280: 297–314.

Schulten, E. A. M., Matysik, J., Alia, Kiihne, S., Raap, J., Lugtenburg, J., Gast, P., Hoff, A. J., and de Groot, H. J. M. (**2002**) ^{13}C MAS NMR and photo-CIDNP Reveal a Pronounced Asymmetry in the Electronic Ground State of the Special Pair of *Rhodobacter sphaeroides* Reaction Centers. *Biochemistry* 41: 8708–8717.

Shkuropatov, A. Y., Khatypov, R. A., Shkuropatova, V. A., Zvereva, M. G., Owens, T. G., and Shuvalov, V. A. (**1999**) Reaction Centers of Photosystem II with a Chemically-Modified Pigment Composition: Exchange of Pheophytins with 13^1-deoxo-13^1-hydroxy-pheophytin *a*. *FEBS Lett* 450: 163–167.

Shkuropatov, A. Y., Khatypov, R. A., Volshchukova, T. S., Shkuropatova, V. A., Owens, T. G., and Shuvalov, V. A. (**1997**) Spectral and Photochemical Properties of Borohydride-Treated D1-D2-Cytochrome b-559 Complex of Photosystem II. *FEBS Lett* 420: 171–174.

van Brederode, M. E., and van Grondelle, R. (**1999**) New and Unexpected Routes for Ultrafast Electron Transfer in Photosynthetic Reaction Centers. *FEBS Lett* 455: 1–7.

van Gorkom, H. J., and Schelvis, J. P. M. (**1993**) Kok′s Oxygen Clock: What Makes it Tick? The Structure of P680 and Consequences of its Oxidizing Power. *Photosynth Res* 38: 297–301.

van Mieghem, F., Brettel, K., Hillmann, B., Kamlowski, A., Rutherford, A. W., and Schlodder, E. (**1995**) Charge Recombination Reactions in Photosystem II. 1. Yields, Recombination Pathways, and Kinetics of the Primary Pair. *Biochemistry* 34: 4798–4813.

van Mieghem, F. J. E., Satoh, K., and Rutherford, A. W. (**1991**) A Chlorophyll Tilted 30 Degrees Relative to the Membrane in the Photosystem II Reaction Center. *Biochim Biophys Acta* 1058: 379–385.

Wakeham, M. C., and Jones, M. R. (**2005**) Rewiring photosynthesis: Engineering Wrong-Way Electron Transfer in the Purple Bacterial Reaction Centre. *Biochem Soc Trans* 33: 851–857.

Ward, H. R., and Lawler, R. G. (**1967**) Nuclear Magnetic Resonance Emission and Enhanced Absorption in Rapid Organometallic Reactions. *J Am Chem Soc* 89: 5518–5519.

Watts, A. (**2005**) Solid-state NMR in Drug Design and Discovery for Membrane-Embedded Targets. *Nat Rev Drug Discov* 4: 555–568.

Webber, A. N., and Lubitz, W. (**2001**) P700: The Primary Electron Donor of Photosystem I. *Biochim Biophys Acta* 1507: 61–79.

Woodbury, N. W., and Allen, J. P. (**1995**) The Pathway, Kinetics and Thermodynamics of Electron Transfer in the Reaction Centers of Purple Nonsulfer Bacteria. *In* Anoxygenic Photosynthetic Bacteria. Blankenship, R. E. and Madigan, M. T. and Bauer, C.E., eds., Kluwer Academic Publishing, Dordrecht, pp 527-557.

Zech, S. G., Olejniczak, E., Hajduk, P., Mack, J., and McDermott, A. E. (**2004**) Characterization of Protein-Ligand Interactions by High-Resolution Solid-State NMR Spectroscopy. *J Am Chem Soc* 126: 13948–13953.

Zouni, A., Witt, H. T., Fromme, P., Krauss, N., Saenger, W., and Orth, P. (**2001**) Crystal structure of Photosystem II from *Synechococcus elongatus* at 3.8 Å resolution. *Photosynth Res* 409: 739–743.

Zysmilich, M. G., and McDermott, A. (**1994**) Photochemically Induced Dynamic Nuclear Polarization in the Solid-State ^{15}N Spectra of Reaction Centers from Photosynthetic Bacteria *Rhodobacter sphaeroides* R26. *J Am Chem Soc* 116: 8362–8363.

Zysmilich, M. G., and McDermott, A. (**1996a**) Photochemically Induced Nuclear Spin Polarization in Bacterial Photosynthetic Reaction Centers: Assignments of the ^{15}N SSNMR Spectra. *J Am Chem Soc* 118: 5867–5873.

Zysmilich, M. G., and McDermott, A. (**1996b**) Natural Abundance Solid-State Carbon NMR Studies of Photosynthetic Reaction Centers with Photoinduced Polarization. *Proc Natl Acad Sci USA* 93: 6857–6860.